Classical growth of hard-sphere colloidal crystals

Bruce J. Ackerson
Department of Physics and Center for Laser Research, Oklahoma State University, Stillwater, Oklahoma 74078-0444

Klaus Schätzel*
Institut für Physik, Johannes Gutenberg-Universität, D-55099 Mainz, Germany
(Received 21 September 1994; revised manuscript received 17 July 1995)

The classical theory of nucleation and growth of crystals is examined for concentrated suspensions of hard-sphere colloidal particles. The work of Russel is modified, extended, and evaluated, explicitly. Specifically, the Wilson-Frenkel growth law is modified to include the Gibbs-Thomson effect and is evaluated numerically. The results demonstrate that there is a critical nucleus radius below which crystal nuclei will not grow. A kinetic coefficient determines the maximum growth velocity possible. For large values of this coefficient, quenches to densities above the melting density show interface limited growth with the crystal radius increasing linearly with time. For quenches into the coexistence region the growth is diffusion limited, with the crystal radius increasing as the square root of elapsed time. Smaller values of the kinetic coefficient produce long lived transients which evidence quasi-power-law growth behavior with exponents between one half and unity. The smaller kinetic coefficients also lead to larger crystal compression. Crystal compression and nonclassical exponents have been observed in recent experiments. The theory is compared to data from small angle scattering studies of nucleation and growth in suspensions of hard colloidal spheres. The experimental nucleation rate is much larger than the theoretically predicted value as the freezing point is approached but shows better agreement near the melting point. The crystal growth with time is described reasonably well by the theory and suggests that the experiments are observing long lived transient rather than asymptotic growth behavior.

PACS number(s): 64.70.Dv, 81.10.Fq, 82.70.Dd

I. INTRODUCTION

It is now widely known that suspensions of colloidal particles undergo phase transformations analogous to that observed in atomic and molecular systems [1,2]. These suspensions are pseudo-one-component systems where the suspended particles are the "atoms" and the suspending solvent remains neutral, i.e., remains in the same thermodynamic state throughout any phase transformation of the particles. Crystallization, the disorder-to-order transition, from a metastable fluid to a crystalline solid has been observed in a variety of systems such as dilute charge stabilized particle suspensions that form bcc crystals similar to a Wigner crystal, more concentrated charge stabilized particle suspensions that form fcc crystals, crystallization to close packed structures driven by attractive depletion flocculation, and sterically stabilized particle suspensions that exhibit "hard-sphere" crystallization [2]. While these studies focus on homogeneous nucleation, a number of other studies have investigated heterogeneous nucleation near cell walls [3,4].

Colloidal suspensions differ from pure atomic systems in that the sample volume is fixed by the solvent, and crystallization occurs at fixed volume rather than fixed (osmotic) pressure. The metastable fluid state, which is generally created by shear melting the sample [5] rather than undercooling, is at a higher osmotic pressure than the final crystalline state or coexisting crystal and liquid state. Because the particles exchange energy and momentum with the solvent, only particle conservation should govern the large time dynamics of the system. This conservation law is expressed as a diffusion equation for the particle dynamics, where a general diffusion tensor [6] may be included to account for solvent mediated hydrodynamic interactions. Furthermore, the relatively small number of colloidal particles in a typical sample (10^{-9} mol) and the rapid exchange of energy with the solvent, means any latent heats evolved or changes in sample temperature are negligible. A heat equation should not be required to describe the system dynamics.

Classical nucleation and growth theories [7–9] have been applied with some success towards understanding these homogeneous nucleation and crystal growth processes [10–13]. Discrepancies between predictions of classical theory and data have often been attributed to lack of knowledge concerning interparticle interactions. However, there are other questions concerning the nature of the crystal growth that have become apparent recently [14]. The work of Aastuen *et al.* on dilute aqueous suspensions of charge stabilized polystyrene particles [10] made direct observations of crystal growth, finding the evolution of crystal sizes to be directly proportional the

*Deceased.

time elapsed after shear melting. This work was interpreted using the classical Wilson-Frenkel growth law. Subsequent work by others on nonaqueous suspensions of charge stabilized silica particles [13,15] implicitly assumed a linear growth law (interface limited growth) in application of the classical theory. However, recent low-angle light-scattering studies on model hard-sphere systems in the solid-liquid coexistence region below the melting volume fraction [16,14] have suggested growth proportional to the square root of the elapsed time (diffusion limited growth), while other similar studies on smaller radii particles suggest growth exponents varying between diffusion and interface limited growth for samples quenched into the equilibrium coexistence region [17].

These different crystal growth exponents are similar to those values found in models for pure atomic systems where crystallization is dependent on the diffusion of heat or impurities away from the interface [18]. For less than unit "undercooling" the growth process becomes diffusion limited with a growth exponent of one half. For greater than unit "undercooling" the growth becomes interface limited and the exponent is unity. Variations from these two limits are essentially produced by relaxation from initial conditions to one limit or the other [19]. We expect to find similar behavior in suitable models for crystallization in colloidal suspensions. The particle motion itself is diffusive in the solvent, and there is a volume fraction difference between the equilibrium liquid and crystal in the coexistence region. Thus a dimensionless undercooling can be defined as the difference between the metastable fluid and fluid freezing volume fractions divided by the difference between the coexisting crystal and fluid volume fractions. A metastable fluid with a volume fraction between these liquid and crystal values corresponds to an undercooling less than unity, while volume fractions greater than the crystal value correspond to values greater than unity.

In this paper the classical theory presented by Russel [13] for the nucleation and growth of hard-sphere colloidal crystals is corrected and extended to study the dynamics of the crystal growth for suspensions of hard colloidal spheres. In the first part of the next section we revise the classical nucleation results presented by Russel to apply to the hard-sphere potential, rather than the truncated Lennard-Jones (inverse twelfth power) potential. Then we introduce collective diffusion within the crystal and metastable liquid and use the Wilson-Frenkel growth law, along with particle conservation and pressure equilibration at the crystal-liquid interface, to determine the motion of the interface. This set of equations is solved numerically to determine crystal size, density, depletion zones, etc., as a function of elapsed time. Results of these simulations are presented in the following section along with a comparison to recently published experimental data.

II. MODEL AND SIMULATIONS

In this section we adapt the classical theories of nucleation and growth to suspensions of hard colloidal spheres. Russel [13] has presented a similar development, which we will follow closely except for the calculation of the excess Gibbs' free energy and the equation of state for the metastable fluid. Furthermore, we will numerically calculate the crystal radius as a function of time rather than assuming a linear growth (constant growth velocity given by the Wilson-Frenkel law) for all undercoolings.

A. Nucleation

The classical theory of homogeneous nucleation [7] expresses the excess Gibbs free energy of a crystallite in terms of bulk thermodynamic quantities as

$$\Delta G^e(r) = 4\pi r^2 \gamma_{f\text{-}s} + (\mu_s - \mu_f)\phi_s (r/a)^3. \tag{1}$$

The first term on the right-hand side represents a contribution from the surface energy of the crystal. It is given by the surface area in terms of the crystal radius, r, times the interfacial tension, $\gamma_{f\text{-}s}$, averaged over all possible orientations of the interface. The equilibrium interfacial tension for hard spheres has been calculated by several different groups. McMullen and Oxtoby [20] calculate an upper limit $\gamma_{f\text{-}s} = 0.425kT/a^2$ for the low-order crystal planes. Curtin [21] finds $\gamma_{100} = 0.165kT/a^2$ and $\gamma_{111} = 0.157kT/a^2$ in a close packed crystal for the low-order planes denoted by the Miller index subscripts. Finally, Marr and Gast [22] find $\gamma_{111} = 0.15kT/a^2$. In these expressions the hard-sphere radius is given by a and the thermal energy by kT. We will assume that the surface tension holds in the metastable region for the nonequilibrium growth process and use the value $\gamma = 0.16kT/a^2$ in subsequent calculations. The second term is the bulk energy of the crystal below that of the same volume of metastable fluid. It is given by the product of the difference in bulk chemical potentials of the crystal (μ_s) and metastable liquid (μ_f) phases times the number of particles in the crystal expressed in terms of the crystal radius. The particle volume fractions of the solid and metastable fluid phases are given by ϕ_s and ϕ_f, respectively.

The position, r^*, of the maximum value of ΔG^e, the "barrier to nucleation," gives the size of the critical nucleus as

$$(r^*/a) = 8\pi\gamma_{f\text{-}s}a^2/[3\phi_s(\mu_f - \mu_s)] \tag{2}$$

and the value of the excess free energy at this point is

$$\Delta G^e(r^*) = (4\pi\gamma_{f\text{-}s}a^2/3)(r^*/a)^2. \tag{3}$$

This differs from the form employed by Russel [13], which was adapted from the excess free energy given by Cape, Finney, and Woodcock [23] for a soft inverse twelfth power potential. We utilize the above form because the growth law also is expressed in terms of chemical potentials, and a single expression for the chemical potential difference can be employed in the same form for both nucleation and growth formulations. However, given the above form for ΔG, we follow Russel and express the equilibrium rate of nucleation by

$$N = \beta\Phi[D_s(\phi_f)/a^5]\phi_f^{5/3}\exp[-\Delta G^e(r^*)/kT], \quad (4)$$

where $D_s(\phi_f)$ is the self-diffusion constant of a particle in the metastable fluid phase and β is a constant assumed to be of order unity. This rate is simply a Boltzmann probability for being at the barrier to nucleation times a kinetic coefficient for crossing the barrier.

Expressions for the chemical potential in the stable and metastable regions may be found following the method outlined by Russel [13]. The Helmholtz free energy per particle takes the form

$$A/kT = \int Z(\phi)(d\phi/\phi) + c. \quad (5)$$

Here $Z(\phi) = \Pi/nkT$ is the ratio of the (osmotic) pressure Π to the product of the thermal energy and the particle number density n. This reproduces the pressure $\Pi = -(\partial NA/\partial V)_{T,N}$ if the constant c is independent of the sample volume V. Since the constant in Eq. (5) must be independent of $\phi = Nv_0/V$, it must also be independent of the number of particles N. Here v_0 is the volume per particle. Then the following expression for the chemical potential μ follows from its definition in terms of the Helmholtz free energy, $\mu = (\partial NA/\partial N)_{T,V}$ as

$$\mu/kT = \int Z(\phi)(d\phi/\phi) + Z(\phi) + c. \quad (6)$$

To evaluate the above expression for the chemical potential requires explicit values for the hard-sphere equation of state. Then the critical nucleus size and nucleation rate may be evaluated using these results. Woodcock [24] has produced equation of state data for the metastable hard-sphere fluid phase with $\phi_f > 0.494$. These data are fit well by the Carnahan-Starling equation [25] and by the following simpler analytic expression in the metastable region:

$$\Pi/nkT = Z(\phi_f) = 0.904/[(\phi_f - 0.731)^2 + 0.0160]. \quad (7)$$

There are other more recent approximations [26] for the metastable fluid, but a preliminary testing of these results produced essentially the same results. Neither Russel nor van Duijneveldt and Lekkerkerker [27], who have made similar calculations, used approximations for the metastable fluid in their calculations. Rather, they used an analytic approximation for the equation of state of the hard-sphere glass. This equation of state was given by Woodcock, as well, and is valid for volume fractions greater than that for the kinetic glass transition ($\phi_f > 0.58$). The equation of state for a face-centered cubic crystal of hard spheres has been determined by computer simulation by Hall [28] and is approximated well by the following equation:

$$\Pi/nkT = Z(\phi_f) = 2.17/(0.738 - \phi_s). \quad (8)$$

For coexisting crystalline solid and metastable fluid phases with $\phi_f > 0.494$, equal pressures enforce the following relation between solid and liquid volume fractions

$$\phi_s = 0.307\phi_f/(\phi_f^2 - 1.05\phi_f + 0.550). \quad (9)$$

When the fluid volume fraction is equal to the freezing value ($\phi_f = 0.494$), this relation gives $\phi_s = 0.546$, the melting value for the coexisting solid phase in computer simulations [29].

Explicit expressions for the chemical potential of solid or liquid phases as a function of volume fraction are determined by substitution of Eqs. (8) or (7) into Eq. (6), respectively. The unknown constant, c, is determined by requiring that the fluid at $\phi_f = 0.494$, the freezing value, have the same chemical potential and pressure as the solid at $\phi_s = 0.546$, the melting value. The difference in chemical potentials between the liquid and crystal phases is found to be

$$\begin{aligned}\Delta\mu(\phi_f,\phi_s)/kT = [\mu_s(\phi_s) - \mu_f(\phi_f)]/kT = &-11.137 - 0.904/(0.551 - 1.46\phi_f + \phi_f^2) - 1.643\ln[\phi_f] \\ &+0.821\ln[0.551 - 1.462\phi_f + \phi_f^2] - 9.492\arctan[7.91(\phi_f - 0.731)] \\ &+2.17/(0.738 - \phi_s) - 2.940\ln[0.738 - \phi_s] + 2.940\ln[\phi_s]. \quad (10)\end{aligned}$$

To complete the evaluation of the nucleation rate, expressions for the self-diffusion constant are required. Russel [13] has developed the following approximations from the published literature [30–33]:

$$D_s^0/D_0 = (1 - \phi_f/3.7)(1 - \phi_f/0.64) \quad (11)$$

and

$$D_s^\infty/D_0 = (1 - \phi_f/2.7)(1 - \phi_f/0.58). \quad (12)$$

Equation (11) approximates the "short time" self-diffusion where mobility is reduced by hydrodynamic interactions with force free neighbors. Russel has enforced two limits in his approximation: $D_s^0/D_0 = 1 - 1.83\phi_f$ as $\phi_f \to 0$ and $D_s^0 \to 0$ as $\phi_f \to 0.64$ at random close packing [31]. At long times the translation of a particle produces a distortion of the equilibrium structure which modifies the self-diffusion with additional retardation. This approximation satisfies the following limiting behavior: $D_s^\infty/D_0 = 1 - 2.1\phi_f$ as $\phi_f \to 0$ and $D_s^\infty \to 0$ as $\phi_f \to 0.58$ at the glass transition.

Recently van Duijneveldt and Lekkerkerker [27] have given different approximations for the short and long time diffusion constants as

$$D_s^0/D_0 = (1 - \phi_f/0.64)^{1.17} \tag{13}$$

and

$$D_s^\infty/D_0 = (1 - \phi_f/0.58)^{1.74}, \tag{14}$$

respectively. The short time expression satisfies the low-density limit and yields results similar to Russel's. The long time expression results from a fit to the data of van Blaaderen *et al.* [34] and Bartsch *et al.* [35] for volume fractions less than the freezing value and from forcing the diffusion constant to zero at the glass transition. Because this form results from a fit to data, it is probably more accurate than the one given by Russel. It is not clear if any of these approximations are valid on the crystal growth time scale or for the nonequilibrium conditions associated with crystallization. In the absence of more detailed information we have these approximations available for use.

B. Growth

Gibbs [36] noted that the surface tension on a small crystal in equilibrium will lead to a lower melting temperature than that for bulk crystal. This "Gibbs-Thomson" correction is included in many theories of crystal growth [37]. For hard-sphere systems, however, temperature is not a relevant parameter, and surface tension leads to a larger pressure exerted on small crystals compared to large ones in the same metastable fluid. Thus larger "undercooling" or compression is needed to stabilize smaller crystals. This effect is included through a pressure balance at the crystal-liquid interface as

$$\Pi(\phi_s) = \Pi(\phi_f) + 2\gamma_{f\text{-}s}/R, \tag{15}$$

where the left-hand side represents the pressure in the crystal and the right-hand side gives the pressure in the fluid plus a pressure increment due to surface tension for an assumed spherical crystal of radius R.

Once a stable crystal has been nucleated, it will grow. The classical Wilson-Frenkel growth law is given by [8,7,13]

$$dR/dt = \alpha[D_s(\phi_f)/2a] \times\{1 - \exp[\Delta\mu/kT + (8\pi\gamma_{f\text{-}s}a^3/3\phi_s R)/kT]\}. \tag{16}$$

This theory assumes the growth of crystallites by the addition of individual molecules (colloidal particles) from the melt. As defined in Eq. (10), $\Delta\mu$ is the difference in chemical potentials between the metastable liquid and the crystal in the immediate vicinity of the interface. The term following the chemical potential difference in the exponent has been added to account for the increased free energy of a finite-sized crystal with surface tension. This term is included to be consistent with Eq. (2). When a crystal has the size of a critical nucleus, this term cancels the chemical potential difference term, giving zero growth velocity. This is consistent with a critical nucleus being in unstable equilibrium with the metastable fluid. For sufficiently large radii crystals this surface energy term is negligible, giving the standard Wilson-Frenkel law. $D_s(\phi_f)$ is a self-diffusion constant applicable on the scale of the interparticle separation. Russel divides the diffusion constant by the particle diameter to find an estimate of the kinetic coefficient in units of velocity. van Duijnevelt and Lekkerkerker [27] use the particle density to set the length scale and find essentially the same values for the volume fraction range of interest. The prefactor α is unknown but dimensionless and assumed of order unity. As mentioned above, it has been assumed that growth velocities were constant in time and Eq. (16) was used to estimate magnitudes [13,15]. This assumption need not be true, as we will show by explicit numerical calculation.

Because the crystal in the coexistence region is more dense than the metastable fluid or the final fluid density, crystal growth will produce a depletion region in the immediate vicinity of the crystal-liquid interface. As a result of this reduced particle density, particles will diffuse into this region from the metastable fluid. If the addition to the crystal results in a nonuniform crystal density, then the crystal will also relax to uniform density via diffusion. These diffusion processes are represented by

$$\partial\phi_f/\partial t = \nabla \cdot D_c^f(\phi_f)\nabla\phi_f, \tag{17}$$

$$\partial\phi_s/\partial t = \nabla \cdot D_c^s(\phi_s)\nabla\phi_s. \tag{18}$$

This diffusion in either phase should be governed by a collective or mutual diffusion constant, and D_c represents such a constant for each phase as a function of the volume fraction for that phase. For hard spheres, experimental results indicate that D_c^f is nearly independent of volume fraction for small fluctuations in the particle density [38–40]. Thus, we will assume for the purposes of our calculations that it is given exactly by the dilute solution value D_0. We have no experimental determination of a mutual or collective diffusion constant for the crystal phase. For simplicity we assume it to be approximately given by the dilute solution value D_0, as well. This may be an overestimate because the compressibility of the solid phase is reduced compared to the liquid and hydrodynamic drag forces are about the same as fluid values [41]. The self-diffusion constants do depend on volume fraction, as evidenced by the approximations given in Eqs. (11)–(14). For the small volume fraction ranges sampled during crystallization, however, we will assume the value to be essentially constant (whatever the value is). With these approximations the equations governing the crystal growth are written in the dimensionless form as

$$\phi_s Z(\phi_s) = \phi_f Z(\phi_f) + 4\pi K/3X, \tag{19}$$

$$dX/d\tau = \delta[1 - \exp(\Delta\mu/kT + 4\pi K/3\phi_s X)], \tag{20}$$

$$\partial\phi_s/\partial\tau = \nabla'^2\phi_s, \tag{21}$$

$$\partial\phi_f/\partial\tau = \nabla'^2\phi_f. \tag{22}$$

In deriving Eq. (19), note that $\phi = 4\pi a^3 n/3$. The resulting dimensionless variables are $\tau = D_0 t/l^2$, $X = R/l$, and $\nabla' = l\nabla$. The parameter $\delta = \alpha l D_s(\phi_f)/2aD_0$, as stated above, is assumed constant and we must assume some fixed value for ϕ_f. In this work we will use the initial value of the metastable fluid. This results in values that give reasonable agreement with data in the range 0.05 to unity. The parameter K is given by $(2\gamma_{f\text{-}s}a^2/kT)a/l$. The particle radius is given by a, and l is any convenient length used to scale space. This length may be identified with the particle radius a or a dimension set by the nucleus number density. We find it convenient in what follows to identify l with the initial nucleus size.

These dimensionless growth equations are solved numerically in one dimension assuming spherical symmetry with growth in only the radial direction. A one-dimensional adaptive grid (having 50–60 points, typically) is referenced to and follows the interface. The grid spacing increases geometrically with increasing distance from the interface. This is done to accommodate the larger spatial variations in particle volume fraction in the immediate vicinity of the interface and to optimize the speed of the computation. Each grid point has an associated particle number and volume. Thus the particle volume fraction, osmotic pressure, and chemical potential may be calculated and used to update grid values based on the equations of motion. During one time step a sequence of calculations is made. First, the number of particles associated with each grid point is updated by diffusion, except across the metastable liquid-crystal interface. Then the Wilson-Frenkel law is used to estimate the new interface position, which typically still lies between the last crystal and first liquid grid points. We employ a two-step procedure. First, the Wilson-Frenkel law is employed to calculate the number of particles that undergo liquid-to-solid conversion. Then the interface is moved, changing the volume (and volume fraction) associated with the two grid points adjacent to the interface, until the osmotic pressures calculated from Eqs. (7) and (8) satisfy Eq. (19). If the interface position moves outside the range defined by the grid points adjacent to the interface, the time step is reduced recursively until an acceptable move can be made. In any case, the time step is always sufficiently small that numerical stability of the diffusion process is maintained [42]. If the new interface position becomes too close to one or the other interface grid points, the grid is shifted to recenter at the interface and the grid values are updated.

In addition to the dimensionless parameters δ and K, there are three other parameters to consider in this growth model. The initial volume fraction, ϕ_0, is assumed uniform throughout space and is used to define a dimensionless undercooling, $\Delta = (\phi_0 - \phi_{\text{freeze}})/(\phi_{\text{melt}} - \phi_{\text{freeze}})$, where the volume fraction of the liquid at freezing and the crystal at melting are given by ϕ_{freeze} and ϕ_{melt}, respectively. The crystal nucleus is placed at the origin and has a radius relative to the particle radius given by l/a. Thus we will identify the scale parameter l with the nucleus radius. Finally, the metastable fluid occupies the volume between the crystal and a larger spherical shell with reduced radius $L/l \sim (N_c)^{-1/3}/l$ where N_c represents the crystallite density. Zero particle flux is enforced at the origin and on the outer boundary shell at L/l. Having an outer boundary with a zero flux condition mimics a finite nucleus density where growing crystals eventually compete with one another for that fluid volume fraction in excess of the final equilibrium value.

III. RESULTS

First, the expressions for nucleation of hard-sphere crystals, presented in the previous section, are evaluated and compared with data. The surface tension is assumed to be $0.16kT/a^2$ in all evaluations. Figure 1 shows the critical nucleus radius normalized by the particle radius as a function of the metastable fluid volume fraction. The upper curve is an evaluation of Eq. (2), when the chemical potentials are determined subject to the constraint that critical nucleus and metastable liquid pressures are governed by Eq. (19), which includes a pressure increment due to surface tension. The lower curve corresponds to the assumption that the crystal and liquid pressures are equal, producing the result given in Eq. (9). The inclusion of the surface tension results in an increase in the crystal volume fraction of approximately 0.002 over that without. The resulting change in chemical potential is more dramatic, with the result that the upper curve is approximately twice the value of the lower. The data shown are from the small angle light-scattering studies of Schatzel and Ackerson [14] where the smallest mea-

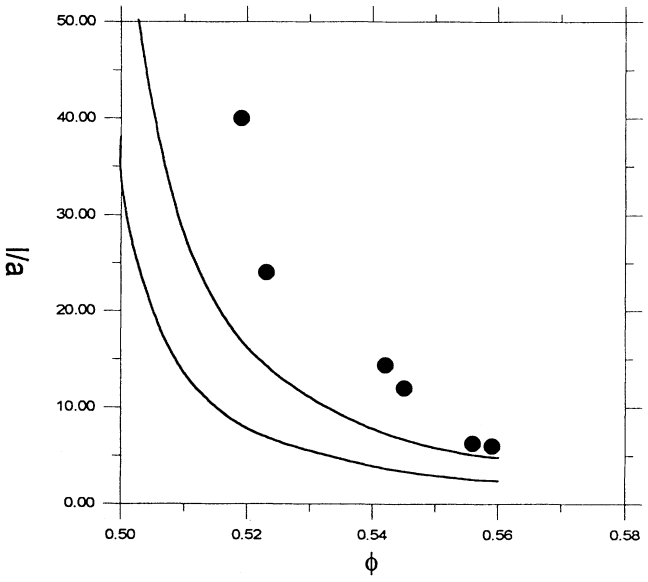

FIG. 1. Reduced nucleus radius as a function of the metastable fluid volume fraction. The upper curve results from an evaluation of Eq. (2) including the Gibbs-Thomson effect. The lower curve is an evaluation of Eq. (2) with equal osmotic pressures on the crystal and fluid. The symbols are the minimum crystal sizes observed in small angle light-scattering experiments, as described in the text.

sured crystal size (determined as described in that paper) is given as a function of volume fraction. The minimum measured sizes are larger than the predicted critical nucleus size at the same volume fraction, although at larger volume fractions they are only marginally greater than the values determined with inclusion of the Gibbs-Thomson effect. These data need not correspond to the critical nucleus size but do represent an upper limit on size. In all cases the crystal size is expected to diverge at the freezing point, where the chemical potentials become equal.

Figure 2 shows the reduced nucleation rate density

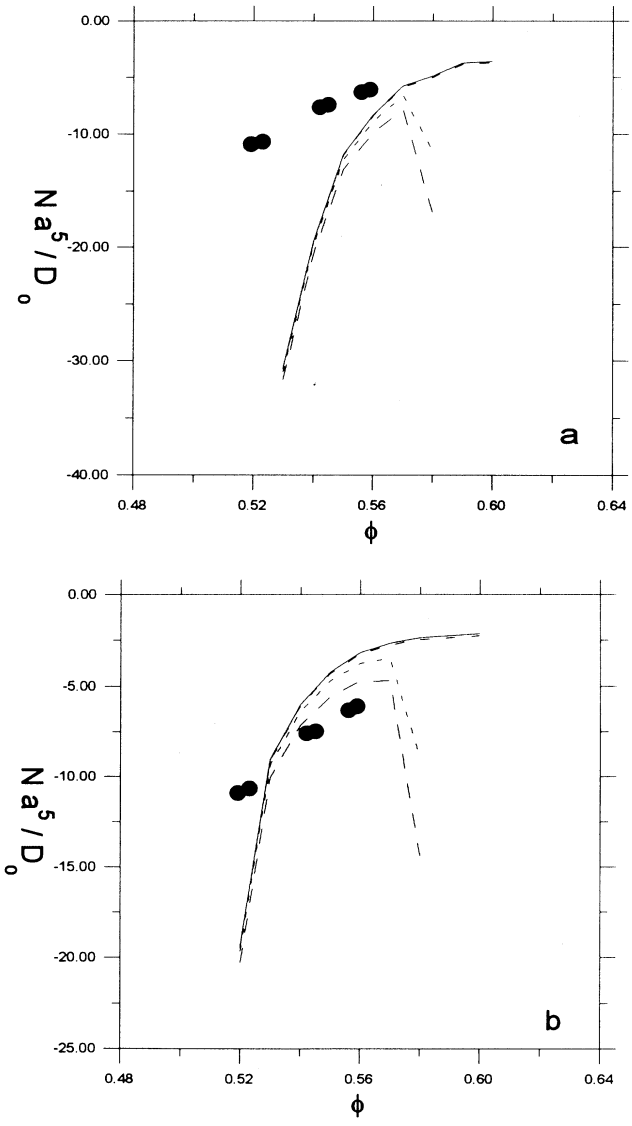

FIG. 2. Logarithm of the reduced nucleation rate density as a function of metastable fluid volume fraction (a) with the Gibbs-Thomson effect included and (b) without. The solid and dashed curves represent from top to bottom results for the different self-diffusion constant given by Eqs. (11), (13), (12), and (14), respectively. For all curves $\beta = 1$. The symbols are data taken from Ref. [14].

presented in Eq. (4) for the different self-diffusion constants given in Eqs. (11)–(14). Figure 2(a) includes the Gibbs-Thomson surface pressure effect and Fig. 2(b) does not. All curves set β to unity. Inclusion of the Gibbs-Thomson effect means that relatively larger nuclei radii are required. This greatly reduces the probability that nuclei will be formed. The data are taken directly from Schatzel and Ackerson [14] and put into dimensionless form for presentation here. The data agree reasonably well with the equal pressure theory using the long time self-diffusion constant given in Eq. (14). The discrepancy is largest as the freezing point is approached, where the experimental nucleation rate density is much larger than predicted theoretically. It is often found that classical nucleation rates require rather large corrections through the parameter β [9]. Even with this freedom of adjustment, the equal pressure form gives the best description of the data because the dependence of the rate on volume fraction is weaker than the rate including the Gibbs-Thomson effect.

Before comparing the data of Schatzel and Ackerson [14] with the growth theory, we first look at the more general features of the model. Five parameters characterize the growth model and produce a large parameter space to explore. We simplify this exploration as follows. First, the spatial scaling parameter l is taken to be the initial nucleus size. Thus the dimensionless crystal radius is $X = R/l = 1$ at $\tau = 0$. Second, the finite nucleus density, which determines the dimensionless position, L/l, of the outer boundary, influences the growth dynamics only at large times as the system approaches equilibrium. For these general investigations of the model, we take this boundary position large enough that little effect due to finite nucleus density is seen. For example, the outer boundary at L/l was placed at 250, 100, and 80 (and also 800) for undercoolings 0.115, 0.885, and 1.27, respectively. Third, to study the asymptotic growth behavior, the parameter K is set to zero. This eliminates any early time dependencies due to the Gibbs-Thomson effect. Once the asymptotic behavior is established, this assumption can be relaxed. Finally, the growth is explored as a function of undercooling Δ from 0.115 to 1.88, and the dimensionless growth velocity δ from 0.001 to 10.

For large values of δ, when the crystal volume fraction is nearly uniform and near the equilibrium value, asymptotic growth laws are evidenced. Figure 3 presents the instantaneous growth exponent $\eta = d \log[X]/d \log[\tau]$ as a function of the reduced time τ for largest dimensionless growth velocities, $\delta = 10$, and a range of undercoolings. A time-independent value for η indicates a power-law growth as $X \sim \tau^{\eta}$. It is seen that the early time growth of the crystals represented in Fig. 3 is not power-law growth but approaches this behavior asymptotically at large times. Similar to results for atomic systems the value of η approaches unity for undercoolings greater than unity and one half for undercoolings between zero and unity. For undercoolings near unity the approach to the final asymptotic value is slow. The run at $\Delta = 1.08$ approaches $\eta = 2/3$ before breaking off and approaching unity at larger times (not shown).

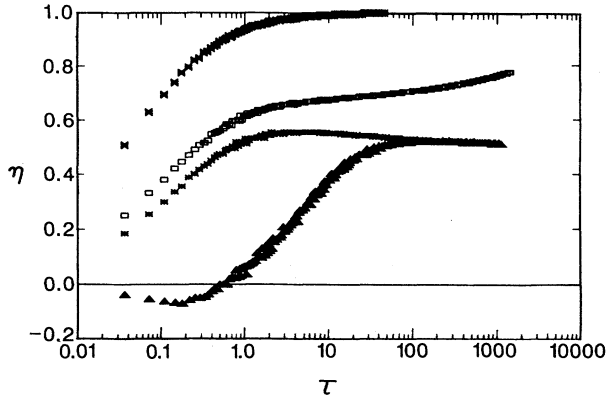

FIG. 3. The instantaneous growth exponent η as a function of reduced time τ for undercoolings $\Delta = 1.88, 1.08, 0.885$, and 0.115 from top to bottom.

At unit undercooling, some growth models are shown to have $\eta = 2/3$ [18].

Figure 4 shows the large time linear power law growth for undercoolings greater than unity, $\Delta = 1.08, 1.27, 1.46, 1.65$, and 1.88. Also shown as lines is the predicted growth law behavior based on the Wilson-Frenkel equation with $K = 0$, a crystal volume fraction equal to the initial metastable fluid value, and a metastable fluid volume fraction in the depletion zone adjacent to the crystal interface consistent with Eq. (9). It is seen that the Wilson-Frenkel law gives a good representation of the growth in this limit. For quenches into the coexistence region giving diffusion limited growth, the proportionality constant in the growth law increases by nearly an order of magnitude in going from $\Delta = 0.115$ to $\Delta = 0.885$. This is predicted by the diffusion limited model of Frank [43], but the absolute values of these numbers are approximately half those values predicted by Frank theory.

Figure 5 shows values of the volume fraction of a growing crystal at its center, $\phi_s(0)$, and at the interface, $\phi_s(X)$, as well as the liquid at the interface, $\phi_f(X)$, and at the outer boundary, $\phi_f(L/l)$, as a function of τ for two different dimensionless growth velocities, $\delta = 10$ and 0.001, and an undercooling $\Delta = 0.885$ (an initial volume fraction for the metastable fluid equal to 0.54). It is observed that $\phi_f(L/l)$ remains constant and equal to the initial undercooling value until the largest time values when it begins a decrease to the equilibrium fluid value. The crystal and liquid interface values are time dependent but maintain a fixed separation with respect to one another, because the osmotic pressure is equilibrated across the interface ($K = 0$). The initial nucleus with the same volume fraction as the metastable fluid has a lower osmotic pressure and is compressed immediately at the surface. This compression eventually is felt at the center of the crystal and also creates a depletion zone

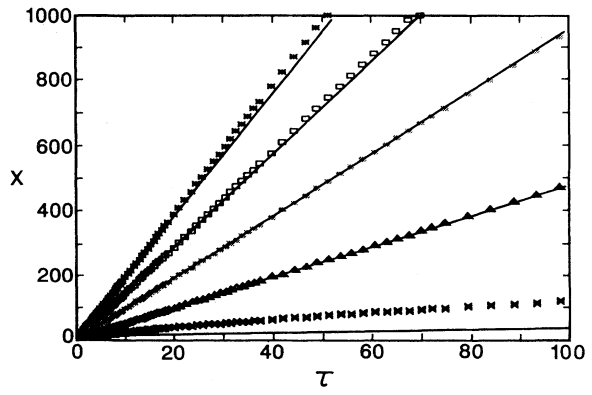

FIG. 4. Reduced crystal radius X as a function of reduced time τ for undercoolings $\Delta = 1.88, 1.65, 1.46, 1.27$, and 1.08 from top to bottom. The solid lines indicate the predicted results from the Wilson-Frenkel grow law evaluated as described in the text.

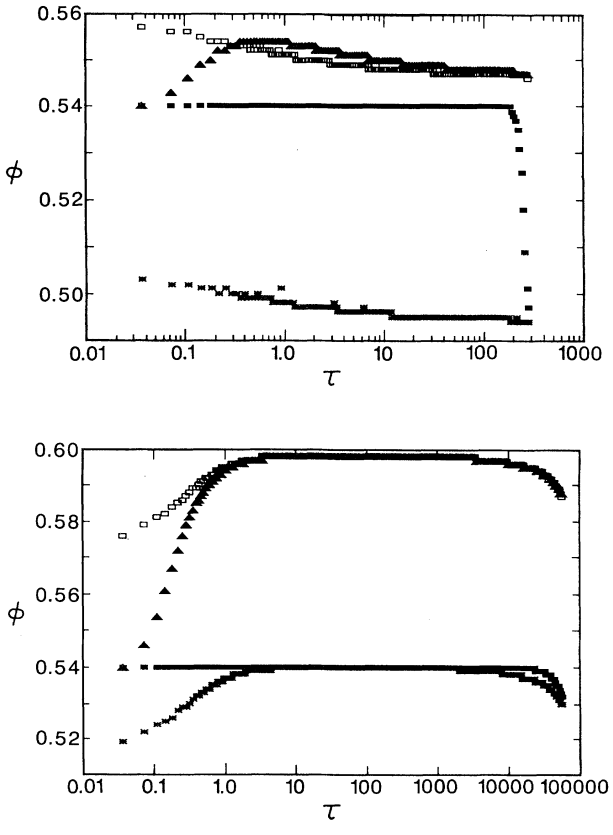

FIG. 5. Volume fraction values in the center of a growing crystal (filled triangles), on the crystal side of the interface (open squares), on the liquid side of the interface (asterisks) and in the liquid at radius L/l (filled squares) as a function of reduced time for undercooling $\Delta = 0.885$. The dimensionless growth velocity is $\delta = 10$ in (a) and $\delta = 0.001$ in (b).

in the fluid. For $\delta = 0.001$ the growth is slow. Particles that diffuse to the crystal interface fill the depletion zone, raise the osmotic pressure on the crystal, and drive the crystal density to a value consistent with mechanical equilibrium with the metastable fluid, before reducing toward equilibrium values at large τ. For $\delta = 10$ the growth is rapid, particles that diffuse to the interface are quickly incorporated into the crystal, and the liquid side is further depleted. The crystal density relaxes rapidly to nearly the equilibrium values with increasing τ. The same behavior is observed for undercoolings greater than unity, except that the metastable fluid volume fraction and the equilibrium crystal volume fraction values are the same.

We now examine the effect of reducing the magnitude of the dimensionless growth velocity, δ, on the growth process for $K = 0$. Figure 6 shows the reduced crystal radius as a function of reduced time for the two different undercoolings, 0.807 and 1.27, and parametrized by δ. Figure 7 shows the instantaneous growth exponent η as a function of reduced time. The volume fraction at the center of the crystal, $\phi_s(0)$, as a function of reduced time is shown in Fig. 8. Consider first the results for the smaller undercooling. The larger the value of δ the more rapid the approach to the asymptotic power-law growth. This is seen explicitly in Fig. 6(a) in the slope of the growth curves and in Fig. 7(a) where the asymptotic exponent value of 1/2 is approached. Because there is a large volume fraction difference between the growing crystal and metastable fluid, a depletion zone easily develops in the fluid phase adjacent to the interface, as material is incorporated into the crystal. When the depth of the zone is near the freezing volume fraction, local equilibrium is attained. Growth is slowed according to the Wilson-Frenkel growth law, until more material can diffuse into the zone. The growth becomes diffusion limited. The depletion zone grows with the crystal and the shape scales with time as shown analytically by Frank [43]. The growth to a specific size takes more time as δ decreases. However, since the incorporation rate of fluid into crystal is reduced, diffusion is better able to keep up; and the instantaneous growth exponents rise to values greater than 1/2. The maximum value of the growth exponent increases from 1/2 to near unity, as δ is reduced. Since

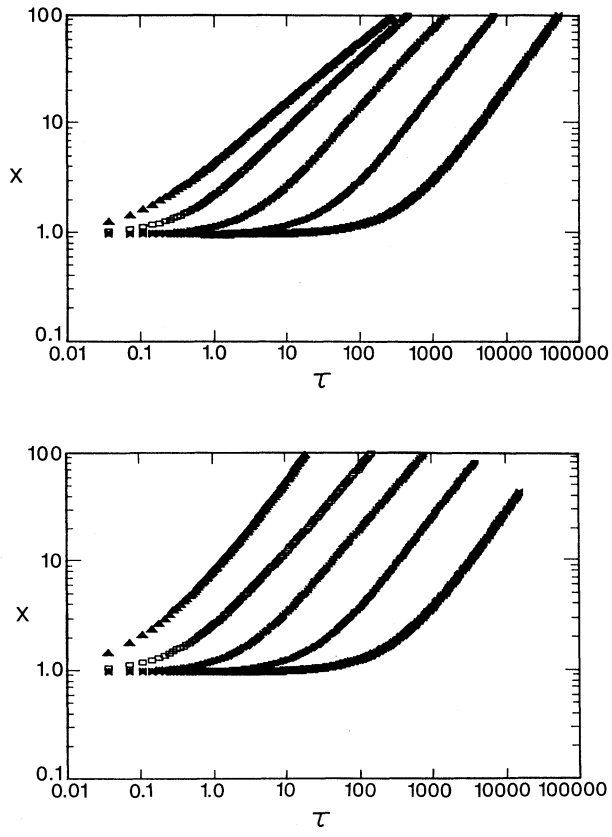

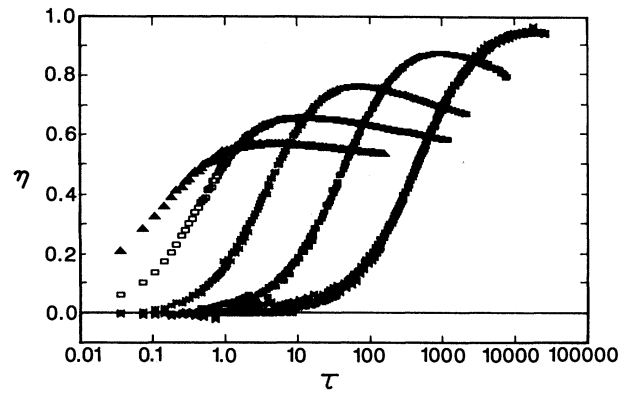

FIG. 6. Reduced crystal radius X as a function of reduced time τ and parametrized by the dimensionless growth velocity, $\delta = 10$, 1, 0.1, 0.01, and 0.001 from left to right. The undercoolings $\Delta = 0.885$ and 1.27 are presented in (a) and (b), respectively.

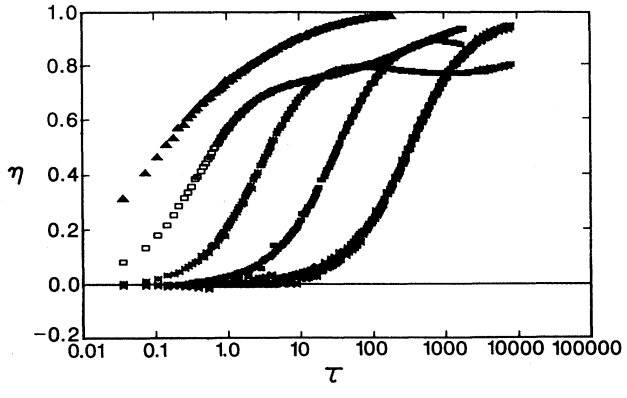

FIG. 7. Instantaneous growth exponent η as a function of reduced time τ and parametrized by the dimensionless growth velocity, $\delta = 10$, 1, 0.1, 0.01, and 0.001 from left to right. The undercoolings $\Delta = 0.885$ and 1.27 are presented in (a) and (b), respectively.

the maximum value is reasonably constant in time, the growth curves in Fig. 6(a) may appear to have power-law behavior. However, growth with exponents greater than 1/2 must eventually lead to diffusion limited growth. The density at the center of the crystal shown in Fig. 8(a) begins the decline from the maximum value roughly when the instantaneous growth exponent exceeds 1/2, the diffusion limiting value. If in experiments the growth time is limited by the nuclei density, then this diffusion limit may not be observed and only larger pseudogrowth exponent transients observed. In summary, the reduced values of δ give rise to longer time transients to diffusion limited growth and larger compression of the crystal.

Figure 6(b) presents results for an undercooling of 1.27. Again, reduced values of δ mean greater times for a crystal to reach a specified size. From Fig. 7(b) it is seen that there is only quasi-power-law behavior, because the growth exponents are changing throughout the growth process. The maximum value of the exponents seen in this figure ranges between 3/4 and unity. This is somewhat puzzling because the metastable fluid volume fraction and the equilibrium crystal volume fraction are the same. There seems to be no reason why fluid cannot be directly converted to crystal, resulting in a linear growth law. In fact, it is possible to solve the growth equations analytically for the case where the crystal and metastable fluid volume fractions are the same. There is an exponentially decaying spatial depletion zone at the interface, which maintains the same decay rate (dependent on the growth velocity) and shape as the crystal radius grows linearly in time. The crystal size and depletion zone do not scale in size together as in diffusion limited growth.

The reason we do not observe exponents of unity in the present model, as δ is reduced, is that local osmotic pressure equilibration compresses the crystal to a higher volume fraction than the final equilibrium value. There is a difference between the crystal volume fraction and the metastable fluid value similar to that observed in the coexistence region for undercoolings less than unity. The growth suffers diffusion limitation, and the instantaneous exponents are less than unity. For the largest δ (= 10) the crystal grows rapidly, and there is little time to compress to much higher volume fraction [Fig. 8(b)]. As a result the instantaneous growth exponent evolves closer to unity than that for the next lower value of δ (= 1.0) examined. For this growth velocity there is increased crystal compression and a resulting larger degree of diffusion limitation, resulting in a growth exponent near 3/4. This curve in Fig. 7(b) does not display a true maximum but rather an inflection. As the crystal volume fraction decays to its equilibrium value, the growth exponent becomes less diffusion limited and evolves towards unity. Further decreasing δ leads to larger local maximum values in the crystal volume fraction. However, if the crystal growth were not limited by the outer boundary, we expect an eventual evolution to interface limited growth with exponent unity, as the crystal volume fraction slowly decays to the equilibrium value. Thus the reduced values of δ again give rise to larger crystal compression and longer lived transients to the expected asymptotic growth behavior.

Finally, we examine in Fig. 9 the Gibbs-Thomson effect on the growth process. In this figure the undercool-

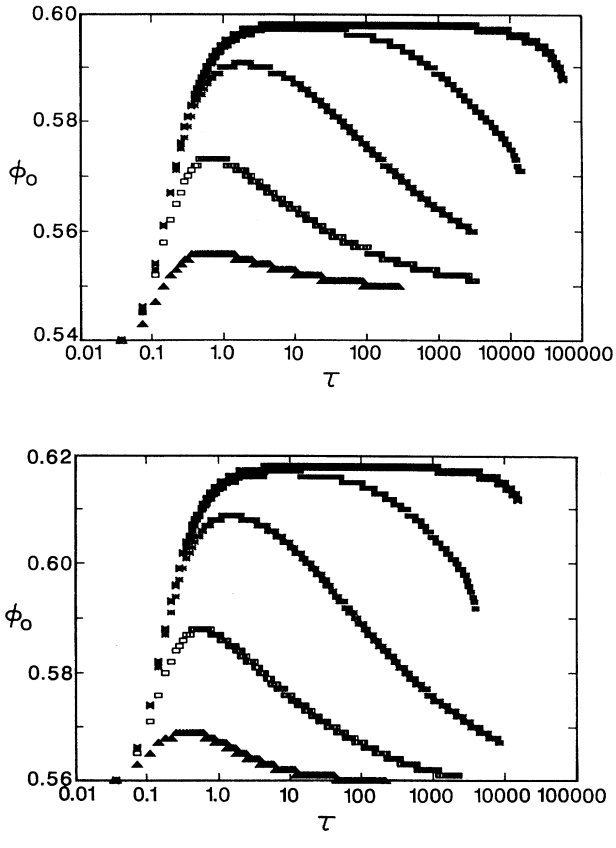

FIG. 8. Volume fraction at the crystal center as a function of reduced time τ and parametrized by the dimensionless growth velocity, $\delta = 0.001, 0.01, 0.1, 1$, and 10 from top to bottom. The undercoolings $\Delta = 0.885$ and 1.27 are presented in (a) and (b), respectively.

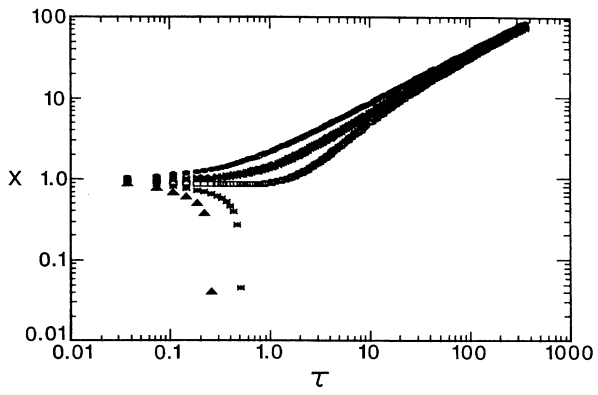

FIG. 9. Reduced crystal radius X as a function of reduced time τ and parametrized by $K = 0, 0.02, 0.03, 0.04$, and 0.05 from top to bottom.

ing is $\Delta = 0.885$ and the dimensionless growth velocity is $\delta = 1$. Curves are plotted for $K = 0.00, 0.02, 0.03, 0.04$, and 0.05. Using the surface tension value $\gamma_{f\text{-}s} = 0.16kT/a^2$ means $K = 0.32(a/l)$. It is seen that a reduced nucleus radius l/a equal to 8.0 or smaller is unstable and decays to zero size, while a radius equal to 10.6 or larger is stable and grows. From Fig. 1 it can be seen that the classical critical nucleus size is 8.8. A slightly larger critical nucleus radius may be required in the growth model than that predicted by classical theory, because the initial crystal having the same density as the metastable fluid is compressed to a smaller radius to balance the external fluid pressure [Eq. (15)] before it can grow. If the radius becomes too small, it collapses to zero size. The uppermost curve corresponds to $l/a = \infty$ or the $K = 0$ result shown previously. The effect of decreasing l/a from infinity is to slow the growth process and further delay the onset of the asymptotic power-law growth behavior. This is another source of instantaneous exponents that deviate from the ideal values of unity or one half.

We now compare the data of Schatzel and Ackerson [14] with the classical crystal growth model presented above. The intensity maximum and characteristic wave vector data show a definite crossover in behavior between the growth and ripening regimes. The crossover time marks the end of the growth process and the crossover size gives the (average) maximum size to which crystals grow. Thus, the crossover size is used to set the outer shell radius, L, in the theory. The critical nucleus radius is determined from the classical theory, and results are generated with and without the Gibbs-Thomson effect. Again l is identified with the nucleus radius and is used to reduce the data. If the critical nucleus size is used in the growth model with the Gibbs-Thomson effect, no growth occurs because the system is in (unstable) equilibrium. Thus, a slightly larger nucleus size leads to the observed growth. In the absence of knowing what size to use, we set $K = 0$ and keep in mind that larger values of K generally mean larger "transient" growth exponents. The data, which represent volume fractions 0.519, 0.523, 0.542, 0.545, 0.556, and 0.559, cluster about three different volume fractions, 0.52, 0.54, and 0.56, which we examine explicitly. The dimensionless growth velocity, δ, is fixed by using the long time self-diffusion result given in Eq. (12) or the short time self-diffusion constant given in Eq. (13). Either of these functions is evaluated at the initial metastable fluid volume fraction. These functions bound a range of possible diffusion constants as Eq. (11) produces values that are larger and Eq. (14) produces values that are smaller than those given by Eqs. (12) and (13). The parameter α is set to unity.

In Fig. 10(a) are shown reduced size, X, versus reduced time, τ, results for growth calculated with the Gibbs-Thomson effect and in Fig. 10(b) without. The solid lines indicate theoretical calculations using values for self-diffusion from Eq. (12) and the dashed lines for self-diffusion from Eq. (13). The symbols are data points determined from the characteristic wave vector in the same manner as for Fig. 1. For volume fraction at 0.52, the two diffusion constant results bound the data with or without inclusion of the Gibbs-Thomson effect in determining the critical nucleus size (value of the reducing parameter l). For volume fraction at 0.54, the results for the smaller critical nucleus size represent the data better and may improve with a larger value choice for the final crystal radius (outer boundary). The fit is not good using the larger critical nucleus value, because the growth is more dominated by transients and is never as steep as the data. It is possible that changing K from zero

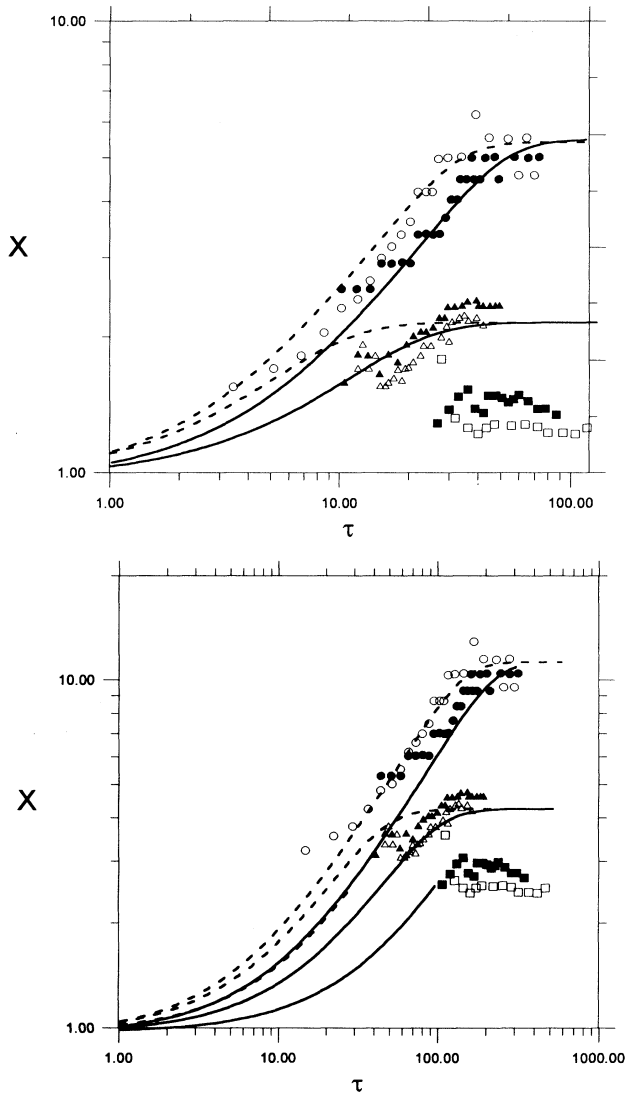

FIG. 10. Reduced crystal radius X as a function of reduced time τ for nucleus radii calculated using the Gibbs-Thomson effect (a) and without (b). The dashed lines represent calculations assuming the self-diffusion constant in δ is given by Eq. (13) and the solid lines assume the self-diffusion is given by Eq. (12). The symbols represent data inferred from Ref. [14], where the volume fractions represented are 0.519 (closed circles), 0.523 (open circles), 0.542 (closed triangles), 0.545 (open triangles), 0.556 (closed squares), and 0.559 (open squares).

would improve the fit, but this has not been explored explicitly. For volume fraction at 0.56, the program failed to converge for the larger critical nucleus value. For the smaller crystal nucleus, the theoretical results are given for a large outer boundary L/l. Because the data indicate no increase in crystal radius, it does not discriminate between results that saturate to this size for values of the reduced time less than 100. These theoretical results indicate the insensitivity of the comparison between theory and experiment in this regard. In fact there may be little growth of nucleated crystals at this volume fraction. The measured crystal size is near the critical nucleus size and shows little growth. However, the scattered intensity is increasing, indicating an increase in the number, if not size, of the scattering centers. Thus this may be purely a nucleation dominated process, which will be explored elsewhere [44].

Finally we note that Schatzel and Ackerson [14] compared X_c^2/τ_c with the dilute solution diffusion constant and with short and long time self-diffusion constants given by Russel. These data are bounded by the diffusion constants but not represented well by any one of them. However, we see in the growth model presented here that the self-diffusion constants give a good representation of the data. Evidently, effects associated with crystal compression, finite-size effects, transient decay effects, etc. must be included for proper description of the growth process.

IV. DISCUSSION

Hard spheres are one of the basic model systems in statistical mechanics. Due to the form of the interparticle interaction, equilibrium properties are independent of temperature and dependent only on particle concentration. The order-disorder transition is entropy driven. For volume fractions greater than the melting value, the disordered metastable fluid has a lower entropy than the equilibrium crystalline state. (Entropy increases in a thermodynamically isolated system, as it approaches equilibrium). While this behavior of the entropy seems contradictory to standard intuition, it can be established from the equations of state for the crystal and metastable fluid determined via computer simulations. These equations of state may also be used to evaluate classical theories of nucleation and growth for hard spheres. Due to the importance of both the hard-sphere model system and the nucleation and growth of crystals, it is important to test these ideas with an experimental realization of a collection of hard spheres. This has been done here.

The growth calculations indicate some general results. When the system is quenched into the coexistence region, diffusion limited growth is approached asymptotically. When the undercooling is greater than unity, interface limited growth is approached asymptotically. Relatively large growth velocities or kinetic coefficients in the Wilson-Frenkel growth law produce a faster approach to asymptotic behavior than small velocities. During this transient relaxation to asymptotic values, quasi-power-law growth with nonclassical exponents may be observed. Inclusion of the Gibbs-Thomson effect produces further modifications of the growth characteristics. The initial crystal size becomes an important parameter, and the stability of nuclei can be examined.

The minimum crystal size measured by Schatzel and Ackerson [14] sets an upper limit on the critical nucleus size. The theoretical predictions of nucleus size are less than these measured values and therefore consistent with experiment. Inclusion of the Gibbs-Thomson effect produces nucleus sizes approximately twice that calculated without.

The nucleation rate density predicted by the classical theory is consistent with the data near melting with $\beta \sim 1$ if the Gibbs-Thomson effect is neglected. If the Gibbs-Thomson effect is included, then agreement between theory and experiment requires $\beta \sim 10^{10}$. While this may seem a large correction, it is similar to that found in application of classical nucleation theory to atomic systems [9]. As the freezing point is approached, the theory underestimates the observed nucleation rate density. This region is dominated by thermodynamic effects, and any adjustments to these terms will influence the good agreement between theory and experiment for the critical nucleus size. It is not clear how to correct the theory at this time.

The Wilson-Frenkel growth law gives a good description of the data when the self-diffusion results given in Eqs. (12) and (13) are used to evaluate the kinetic coefficient. While a growth exponent of one half in the coexistence region suggests that asymptotic growth has been achieved, the theory indicates that the observed growth is influenced by a number of factors including finite nucleus density, crystal compression, transient relaxation to asymptotic behavior, etc. Thus the simple estimates of growth parameters given in Ref. [14] are understandably inaccurate, and the classical theory of growth does quite well in describing the data. Furthermore, recent studies of low-order Bragg scattering from similar suspensions indicate that the crystals are compressed as found in our numerical studies [45]. We hope to apply this model to these and other small angle studies in future work.

Finally, we make some comments concerning other models of crystal growth. The crossover from diffusion limited to kinetic limited regimes in crystal growth has been investigated recently in the "phase-field" model of Halperin, Hohenberg, and Ma [46,47] (their "model C"). This model couples an (nonconserved) order parameter field to a conserved quantity having diffusive dynamics. Typically the order parameter represents a measure of the crystalline order. It is attracted to minima in the free energy surface. These minima are at an order parameter value equal to unity (crystal state) or zero (liquid state). Different models for the free energy surface have been examined [18,48]. The conserved quantity for solidification in a pure material is taken to be the temperature and for a metallic alloy the impurity concentration. These two models have been shown to be equivalent mathematically [37]. The long time behavior in these models shows diffusion limited growth when the undercooling is less than unity (into the coexistence region) and interface (kinetics) limited when the undercooling is greater than

unity. For undercoolings greater than unity, the resulting velocity depends on the degree of undercooling and may go to zero at unit undercooling, if the ratio of the "order parameter diffusion constant" to the thermal or impurity diffusion constant is less than a critical value [18]. Otherwise the velocity jumps to a finite value as the undercooling becomes just larger than unity.

It seems that freezing in hard-sphere systems should have a phase-field description. However, temperature is not an important control parameter for hard-sphere systems, and (osmotic) pressure is not a conserved quantity. Fortunately, Caginalp [49] has shown the asymptotic equivalence of the phase-field equations to various Stefan and Hele-Shaw type models that have a sharp interface separating crystal and liquid phases. One limit gives the modified Stefan model. This model comes the closest to the model outlined in this paper, if the conserved parameter is taken to be the particle volume fraction or particle number density. Then one condition on the interface is interpreted as a statement of particle conservation as particles diffuse into the interface and undergo a volume change on freezing or melting. The other condition gives a linear relation between the interface velocity, the interface curvature (Gibbs-Thompson effect), and the volume fraction. The Wilson-Frenkel law can be reduced to a similar linear relation if the argument in the exponent of Eq. (16) is small such that the exponent can be expanded to first order and this linear term expanded in terms of the particle volume fraction. Then there is a direct connection between the two models, but it is a severe approximation. It is not clear at this time if a phase-field model for hard spheres will show, for example, a similar compression and expansion of the crystal during growth.

ACKNOWLEDGMENTS

Travel support through a North Atlantic Treaty Organization Grant No. CRG-920270 is acknowledged. One of us (B.J.A.) acknowledges support through a National Science Foundation Grant No. DMR-9122589. Finally this manuscript has benefited from B.J.A.'s discussions with Bill van Megen and his group.

[1] *Phase Transitions*, Vol. 21, edited by B. J. Ackerson (Gordon and Breach, New York, 1990).
[2] P. N. Pusey, in *Liquids, Freezing and the Glass Transition*, edited by D. Levesque, J. P. Hansen, and J. Zinn-Justin (Elsevier, Amsterdam, 1990).
[3] I. S. Sogami and T. Yoshiyama, in *Phase Transitions* (Ref. [1]), p. 171.
[4] D. G. Grier and C. A. Murray, J. Chem. Phys. **100**, 9088 (1994).
[5] B. J. Ackerson and N. A. Clark, Phys. Rev. Lett. **46**, 123 (1981).
[6] B. U. Felderhof, Physica (Amsterdam) **89A**, 373 (1977).
[7] J. Frenkel, *Kinetic Theory of Liquids* (Oxford University Press, Oxford, 1946).
[8] H. A. Wilson, Philos. Mag. **50**, 238 (1900).
[9] K. F. Kelton, in *Solid State Physics*, Vol. 45, edited by E. Reich and D. Turnbull (Academic, New York, 1991), p. 75.
[10] D. J. W. Aastuen, N. A. Clark, L. K. Cotter, and B. J. Ackerson, Phys. Rev. Lett. **57**, 1733 (1986); **57**, 2772(E) (1986).
[11] K. E. Davis and W. B. Russel, Adv. Ceram. **21**, 573 (1987).
[12] K. E. Davis and W. B. Russel, Ceramic Trans. **1B**, 693 (1988).
[13] W. B. Russel, in *Phase Transitions* (Ref. [1]), p. 127.
[14] K. Schatzel and B. J. Ackerson, Phys. Rev. E **48**, 3766 (1993).
[15] J. K. G. Dhont, C. Smits, and H. N. W. Lekkerkerker, J. Colloid Interface Sci. **152**, 386 (1992).
[16] K. Schatzel and B. J. Ackerson, Phys. Rev. Lett. **68**, 337 (1992).
[17] Y. He, B. J. Ackerson, S. M. Underwood, W. van Megen, and K. Schatzel (unpublished).
[18] H. Lowen, J. Bechhoefer, and L. S. Tuckerman, Phys. Rev. A **45**, 2399 (1992).
[19] R. J. Schaefer and M. E. Glicksman, J. Cryst. Growth **5**, 44 (1969).
[20] W. E. McMullen and D. W. Oxtoby, Phys. Chem. Liq. **18**, 97 (1988).
[21] W. A. Curtin, J. Chem. Phys. **39**, 6775 (1989).
[22] D. W. Marr and A. P. Gast, Phys. Rev. E **47**, 1212 (1993).
[23] J. N. Cape, J. L. Finney, and L. V. Woodcock, J. Chem. Phys. **75**, 2366 (1981).
[24] L. V. Woodcock, Ann. N.Y. Acad. Sci. **37**, 274 (1981).
[25] N. F. Carnahan and K. E. Starling, J. Chem. Phys. **51**, 635 (1979).
[26] J. Tobochnik and P. M. Chapin, J. Chem. Phys. **88**, 5824 (1988).
[27] J. S. van Duijneveldt and H. N. W. Lekkerkerker, in *Science and Technology of Crystal Growth*, edited by J. P. van der Eerden and O. S. L. Bruinsma (Kluwer Academic, Dordrecht, 1995).
[28] K. R. Hall, J. Chem. Phys. **57**, 2252 (1972).
[29] W. G. Hoover and F. H. Ree, J. Chem. Phys. **49**, 3609 (1968).
[30] P. N. Pusey and W. van Megen, J. Phys. (Paris) **44**, 285 (1983).
[31] A. van Veluwen, H. N. W. Lekkerkerker, C. G. de Kruif, and A. Vrij, J. Chem. Phys. **87**, 4873 (1987).
[32] R. H. Ottewill and N. St. J. Williams, Nature **325**, 232 (1987).
[33] W. van Megen and S. M. Underwood, J. Chem. Phys. **91**, 552 (1989).
[34] A. van Blaaderen, J. Peetermans, G. Maret, and J. K. G. Dhont, J. Chem. Phys. **96**, 4591 (1992).
[35] E. Bartsch, V. Frenz, S. Moller, and H. Sillescu, Physica (Amsterdam) **201A**, 363 (1993).
[36] J. W. Gibbs, *Collected Works* (Yale University Press, New York, 1948).
[37] J. S. Langer, Rev. Mod. Phys. **52**, 1 (1980).
[38] M. M. Kops-Werkhoven and H. M. Fijnaut, J. Chem. Phys. **74**, 1618 (1981).

[39] M. M. Kops-Werkhoven and H. M. Fijnaut, J. Chem. Phys. **77**, 2242 (1982).
[40] W. van Megen, S. M. Owens, R. H. Ottewill, and P. N. Pusey, J. Chem. Phys. **82**, 508 (1985).
[41] S. E. Paulin, master thesis, Oklahoma State University, 1989.
[42] W. H. Press, B. P. Flannery, S. A. Teukolsky, and W. T. Vetterling, *Numerical Recipes* (Cambridge University Press, Cambridge, 1986).
[43] F. C. Frank, Proc. R. Soc. London A **201**, 586 (1950).
[44] W. van Megen and B. J. Ackerson (unpublished).
[45] J. L. Harland, S. I. Henderson, S. M. Underwood, and W. van Megen (unpublished).
[46] B. I. Halperin, P. C. Hohenberg, and S. K. Ma, Phys. Rev. B **10**, 139 (1974).
[47] P. C. Hohenberg and B. I. Halperin, Rev. Mod. Phys. **49**, 435 (1977).
[48] H. Lowen, S. A. Schofield, and D. W. Oxtoby, J. Chem. Phys. **94**, 5685 (1991).
[49] G. Caginalp, Phys. Rev. A **39**, 5887 (1989).